

increment that varies randomly in the range ± 100 days. This ensures that our random samples have the same overall distribution of events with time. Actual locations are retained. Using exactly the same procedure as for the real data, we ran 100,000 trials, with a $\pm 1,000$ -day time span, and determined the largest count in the 2,000 bins for each run. The largest count generated in any time bin was 8 (once), so that the probability of getting, by chance, a bin count of 8 with the real data is 10^{-5} ; the data set has a bin count of 11 for the day following the earthquakes. If we consider the event distributions to be poissonian, we reach comparable conclusions.

We have also examined the eruption catalogue for paired eruptions. Figure 2 shows that volcanoes separated by less than 200 km have paired (within two days) eruptions with frequencies much higher than for the background rate. As volcanic earthquakes are usually not large (infrequently as big as magnitude 6), these time–distance characteristics for the enhanced paired eruptions are consistent with our hypothesis that the second eruption is triggered by the passage of seismic waves. (For the time period examined, the earthquake catalogue is not complete, especially for smaller magnitudes, so we cannot identify the triggering earthquakes.)

The interval between eruptions for many volcanoes is usually decades or longer. If the recharge rate of the shallow reservoir is essentially constant with time, then the volcano can be at a near critical level for years. As the Landers earthquake produced an increase in pressure in the magma reservoir under Long Valley at a distance of about 400 km, then the same should be true generally: seismic waves from earthquakes have the potential to increase the pressure in magma chambers even at large distances from large earthquakes. For a volcano already close to the critical pressure state, this could result in a premature eruption. This conclusion is based on secure observations and does not depend on which (if any) of the various models^{5,18–23} proposed is correct, although we note that our suggestion⁵ is the only one that leads naturally to the timescale and character of the observed deformation.

The work emphasizes the need for a programme of continuous deformation monitoring of active volcanoes on a global scale, with sufficient sensitivity to be able to detect deformation transients on these short timescales. We note that a two-colour laser ranging system, with resolution of about 1 mm, was not able to detect changes during the period of triggered seismicity at Long Valley; seismic monitoring is important but gives only indirect information about the deformational changes. Very few active volcanoes are currently monitored well enough to allow detection of potentially important transient deformations. □

Received 14 April; accepted 14 July 1998.

1. Yokoyama, I. Volcanic eruptions triggered by tectonic earthquakes. *Geophys. Bull. Hokkaido Univ.* **25**, 129–139 (1971).
2. Nakamura, K. Volcano structure and possible mechanical correlation between volcanic eruptions and earthquakes. *Bull. Volcanol. Soc. Jpn* **20**, 229–240 (1975).
3. Hill, D. P. *et al.* Seismicity remotely triggered by the magnitude 7.3 Landers, California, earthquake. *Science* **260**, 1617–1623 (1993).
4. Langbein, J., Hill, D. P., Parker, T. N. & Wilkenson, S. K. An episode of reinflation of the Long Valley Caldera, eastern California; 1989–1991. *J. Geophys. Res.* **98**, 15851–15870 (1993).
5. Linde, A. T., Sacks, I. S., Johnston, M. J. S., Hill, D. P. & Bilham, R. G. Increased pressure from rising bubbles as a mechanism for remotely triggered seismicity. *Nature* **371**, 408–410 (1994).
6. Simkin, T. & Siebert, L. *Volcanoes of the World* (Geoscience, Tucson, 1994).
7. Michell, J. Conjectures concerning the cause, and observations upon the phenomena of earthquakes; particularly of that great earthquake of Nov. 1, 1755, which proved so fatal to the city of Lisbon, and whose effects were felt as far as Africa, and more or less throughout almost all of Europe. *Phil. Trans. R. Soc. Lond.* **51**, 566–634 (1760).
8. Guliyas, E., Deak, G. & Hedervari, P. in *Proc. Symp. on Andean and Antarctic Volcanology Problems* (ed. Gonzalez, F. O.) 562–576 (Int. Assoc. Volcanol. and Chem. Earth's Interior, Rome, 1976).
9. Gonzalez, F. O. Volcanic eruption related with great earthquakes as a parameter for forecasting event; the historical cases along the Chilean Andes. *Int. Un. Geodesy and Geophysics, General Assembly Abstr.* Vol. 2, 428 (Vancouver, 1987).
10. Williams, S. N. Erupting neighbors; at last. *Science* **267**, 340–341 (1995).
11. Steinberg, G., Steinberg, A. & Merzhanov, A. Fluid mechanism of pressure growth in volcanic (magmatic) systems. *Mod. Geol.* **13**, 257–265 (1989).
12. Sahagian, D. L. & Proussevitch, A. A. Bubbles in volcanic systems. *Nature* **359**, 485 (1992).
13. Gudmundsson, G. & Saemundsson, K. Statistical analysis of damaging earthquakes and volcanic eruptions in Iceland from 1550–1978. *J. Geophys.* **47**, 99–109 (1980).
14. Newhall, C. G. & Dzurisin, D. Historical unrest at large calderas of the world. *US Geol. Surv. Bull.* **1855**, 19–20 (1988).
15. Global hypocenter data base CD-ROM Version 3.0 (National Earthquake Information Center, US Geological Survey, Denver, 1994).

16. Darwin, C. On the connexion of certain volcanic phenomena in South America; and on the formation of mountain chains and volcanoes, as the effect of the same power by which continents are elevated. *Trans. Geol. Soc. Lond.* **5**, (2nd ser.), 601–631 (1840).
17. Diaconis, P. & Efron, B. Computer-intensive methods in statistics. *Sci. Am.* **248**, 116–130 (1983).
18. Bodin, P. & Comberg, J. Triggered seismicity and deformation between the Landers, California, and Little Skull Mountain, Nevada, earthquakes. *Bull. Seismol. Soc. Am.* **84**, 835–843 (1994).
19. Gomberg, J. & Bodin, P. Triggering of the $M_w = 5.4$ Little Skull Mountain, Nevada, earthquake with dynamic strains. *Bull. Seismol. Soc. Am.* **84**, 844–853 (1994).
20. Anderson, J. G. *et al.* Seismicity in the western Great Basin apparently triggered by the Landers, California, Earthquake, 28 June 1992. *Bull. Seismol. Soc. Am.* **84**, 863–891 (1994).
21. Hill, D. P., Johnston, M. J. S., Langbein, J. O. & Bilham, R. Response of Long Valley caldera to the $M_w = 7.3$ Landers, California, earthquake. *J. Geophys. Res.* **100**, 12985–13005 (1995).
22. Johnston, M. J. S. *et al.* Transient deformation during triggered seismicity from the 28 June 1992 $M_w = 7.3$ Landers earthquake at Long Valley volcanic caldera, California. *Bull. Seismol. Soc. Am.* **85**, 787–795 (1995).
23. Sturtevant, B., Kanamori, H. & Brodsky, E. E. Seismic triggering by rectified diffusion in geothermal systems. *J. Geophys. Res.* **101**, 25262–25282 (1996).

Acknowledgements. We thank T. Simkin for making available the Smithsonian eruption catalogue in digital form.

Correspondence and requests for materials should be addressed to A.T.L. (e-mail: linde@dtm.ciw.edu).

Electric fish measure distance in the dark

Gerhard von der Emde*, Stephan Schwarz*, Leonel Gomez†‡, Ruben Budelli‡ & Kirsty Grant†

* *Institute für Zoologie, Universität Bonn, Poppelsdorfer Schloss, D-53115 Bonn, Germany*

† *Institute Alfred Fessard, C.N.R.S., F-91198 Gif-sur-Yvette, Cedex, France*

‡ *Department of Biomathematics, Faculty of Science, University of the Republic of Uruguay, Montevideo, Uruguay*

Distance determination in animals can be achieved by visual or non-visual cues¹. Weakly electric fish use active electrolocation for orientation in the dark². By perceiving self-produced electric signals with epidermal electroreceptors, fish can detect, locate and analyse nearby objects. Distance discrimination, however, was thought to be hardly possible because it was assumed that confusing ambiguity could arise with objects of unknown sizes and materials^{3–5}. Here we show that during electrolocation electric fish can measure the distance of most objects accurately, independently of size, shape and material. Measurements of the ‘electric image’ projected onto the skin surface during electrolocation^{6–8} revealed only one parameter combination that was unambiguously related to object distance: the ratio between maximal image slope and maximal image amplitude. However, slope-to-amplitude ratios for spheres were always smaller than those for other objects. As predicted, these objects were erroneously judged by the fish to be further away than all other objects at an identical distance. Our results suggest a novel mechanism for depth perception that can be achieved with a single, stationary two-dimensional array of detectors.

For orientation in their environment, animals use sensory information to judge the distance of an object. Disparities in the two retinal images of an object can give stereoscopic depth perception in animals whose eyes have overlapping fields of vision^{9,10}. Other mechanisms for distance discrimination rely on the movement of detectors and successive comparison of images¹¹, on binocular convergence, or on measuring the speed at which objects’ images move across the retina¹². Nocturnally active animals, however, must supplement vision with other senses such as hearing, mechanoreception or olfaction^{13–15}.

Weakly electric fish orient themselves at night by using active electrolocation^{2,16}. By emitting an electric signal (Fig. 1b) with a specialized electric organ, they generate an electric field and perceive the resulting current that flows through epidermal electroreceptors. Nearby objects distort the electric field and alter the current flowing through the electroreceptors⁶. Analysis of the ‘electric image’, that is, the spatial pattern of voltage change, that objects project onto the

skin surface^{7,8} enables a fish to detect and locate objects in complete darkness, and also to assess their electrical properties³. However, unequivocal distance perception was thought not to be possible without auxiliary means, because differences in the sizes and materials of objects could affect the electric image in the same way as differences in distance^{4,17}. In contrast to visual images, which become smaller with an increase in object distance, an increase in distance during active electrolocation leads to a larger size of the electric image¹⁸ and a decrease in its maximal amplitude (intensity) (Fig. 1a). However, a similar but larger object at the same distance would have the same effect. Thus, if fish only measured image size or image amplitude, they should not be able to determine the distances of unknown objects of different sizes.

Experiments were conducted with the weakly electric fish *Gnathonemus petersii*, a nocturnal, stream dwelling predator of insect larvae¹⁹, to find out whether, and how accurately, electric fish can measure object distance. Over a period of 3–5 weeks, three fish were trained to electrolocate two objects according to their distance behind corresponding fixed gates, and to swim through the gate behind which the object was further away (Fig. 1c). Fish alternated between the two gates several times before making a decision, thereby scanning each object with electroreceptor arrays on both the sides of the body and the head.

First, we offered the fish two identical objects, which differed only in their distances from the gate. The distance of the closer object remained fixed in any given trial, defining 'gate distance'. In total, we tested each fish with 12 different combinations of objects, each tested at a minimum of four different gate distances. Discrimination was always correctly achieved provided that inter-object distances differed by more than a critical threshold value (Fig. 2a, b). Discrimination thresholds were correlated with gate distance: fish were better at determining the distances of nearby objects. When gate distances were held constant, thresholds were inversely correlated with object size: distance estimates improved when larger objects were offered.

Because the discrimination of identical objects in different positions could be based on measurements of electric image amplitude or size rather than on object distance, in subsequent experiments we offered the fish two objects that differed in size, shape (for example, a cube and a pyramid) or material (for example, a metal cube and a plastic cube). Twenty-five combinations of different types of object were tested. Differences in these physical parameters did not affect distance discrimination performance (Fig. 2c). Fish could always determine which object was more distant irrespective of size, shape or material of the objects, provided that the distance difference was above the threshold.

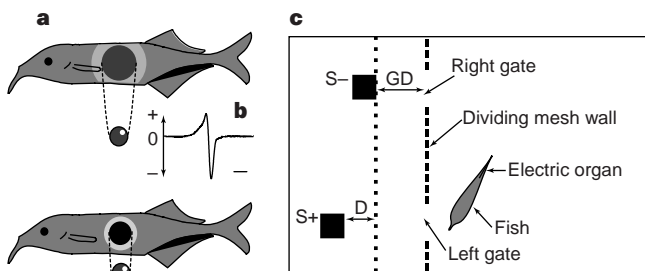


Figure 1 **a**, Electric image size and amplitude change with object distance. Electric images have a 'Mexican hat' profile⁷. An object far from the fish's skin (top) produces a relatively large electrical image with a small amplitude and low edge contrast, indicated by shading. When the same object comes closer (bottom), the size of the image decreases and maximal amplitude and edge contrast increase. **b**, Waveform of the electric organ discharge (EOD) of *Gnathonemus petersii*. Time scale bar equals 100 μ s. **c**, Set-up for behavioural experiments (not drawn to scale). GD, gate distance; D, distance between objects; S+, target object (farther away); S-, non-target object.

To understand which parameters of the electric image are used by fish to determine object distance, we measured the 'electric images' produced locally at the level of the electroreceptors by different objects (Fig. 3a, b). No single physical parameter showed a pattern of variation sufficient to explain distance discrimination⁵. Thus, if the fish had relied only on image size, amplitude or edge contrast, they would have made systematic errors when certain object combinations were offered. But such errors did not occur. Neither could fish have monitored the change of one of these parameters during their approach to the objects^{11,20}, because this would not have provided the fish with unequivocal distance cues when approaching an object of unknown size or impedance⁶. The only parameter combination that could provide a quantitative explanation compatible

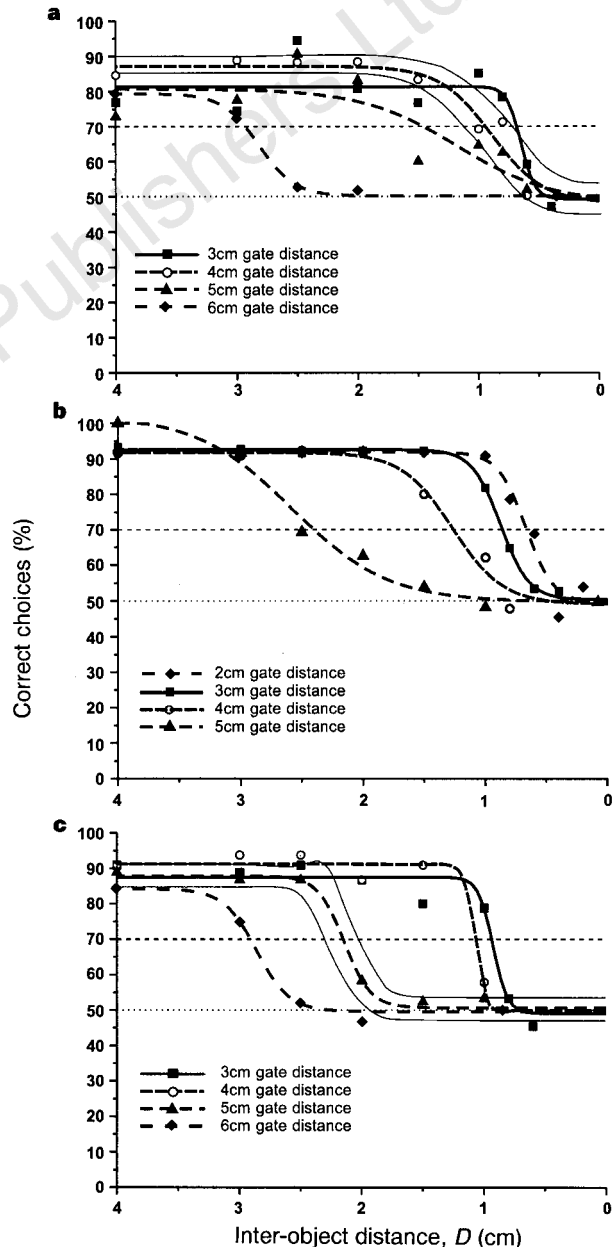


Figure 2 Psychometric functions for distance discrimination of **(a)** two identical metal cubes (64 cm³), **(b)** two identical metal spheres (33.5 cm³) and **(c)** two metal cubes of different sizes (125 and 27 cm³). Discrimination threshold was defined as the inter-object distance D for which the sigmoid function fitted to each data set crossed the 70% correct choice value. Each data point is based on at least 150 trials. In **(a)** and **(c)** thin lines indicate 95% confidence limits for two different curves (4 cm and 5 cm gate distances)³⁰. All curves are significantly different ($P < 0.05$).

with all our behavioural results was the ratio of the maximal slope of the 'electric image' to its maximal amplitude. This slope-to-amplitude ratio depended only on object distance and was independent of size, shape and material for most objects (Fig. 3c, d).

Our measurements also showed that only the rostral slope of the image (the left slopes in Fig. 3b, c) provided adequate information for the fish to determine object distance. The caudal (right) image slopes of different electric images varied unsystematically with object distance, probably because the proximity of the electric organ produces asymmetries in the electric field. Thus, they could not provide any reliable distance cues. We therefore suggest that fish used the rostral image slopes to determine slope-to-amplitude ratios, and thus to determine object distance.

This hypothesis was tested in the following way. Electric image measurements showed that slope-to-amplitude ratios for spheres were smaller than those obtained for solid cubes of the same diameter at the same distance (Fig. 3c, d). The difference in slope-to-amplitude ratios corresponded to a difference in distance of ~1.5 cm at a gate distance of 3 cm (Fig. 3d, arrow). Thus, it was predicted that fish would erroneously judge a sphere to be ~1.5 cm further away than a cube at the same distance.

Experimentally we found this did in fact occur (Fig. 4). Three fish were given the task of comparing the distances of a metal sphere and a metal cube. When the sphere was further away, fish chose it correctly, but they also continued to choose it when both objects were at the same distance. At a 'gate distance' of 3 cm, when the cube was further away, fish started to choose randomly between the two objects at an inter-object distance of ~2 cm. As inter-object distance was further reduced, fish incorrectly chose the sphere instead of the

cube (Fig. 4a). Thus, fish judged the sphere to be farther away than the cube, even through this was not true. The psychometric functions established at a 'gate distance' of 3 cm for distance discrimination of (1) a cube and a sphere and (2) two identical cubes (Fig. 4a) show that the curve for the cube/sphere discrimination crosses the 50% correct line ~1.5 cm closer to larger inter-object distances than that for the two cubes (Fig. 4a, two-headed arrow). Thus, at a 'gate distance' of 3 cm, the sphere seemed to the fish to be ~1.5 cm farther away than the cube as predicted from our electric image measurements (Fig. 3d). Similar 'electrical illusions' also occurred at the other 'gate distances' tested (2 and 4 cm; Fig. 4b), indicating a general mechanism for distance perception.

The results of our experiments suggest that electric fish can measure three-dimensional depth by analysing the electric image of objects projected onto a single, stationary two-dimensional array of electroreceptors. This mechanism differs from all spatial orientation mechanisms shown so far in other species, but resembles a mechanism hypothesized from theoretical postulates of hydrodynamical imaging by the lateral-line system of blind cave fish²¹. Other examples of stationary detector systems include auditory location of a sound source by the cod¹³, surface-feeding fish that determine distance by analysis of the frequency modulation and the curvature of a wave train²², and chameleons, toads and other species, which use the accommodation of their lenses to judge the distance of near objects^{10,23}. Echolocating bats, like electric fish, employ an active location system, but this is based on acoustics. In contrast to electric fish, bats can make time measurements²⁴ and thus can determine object distance by employing temporal cues²⁵⁻²⁷. The mechanism proposed for distance measurement in electric fish

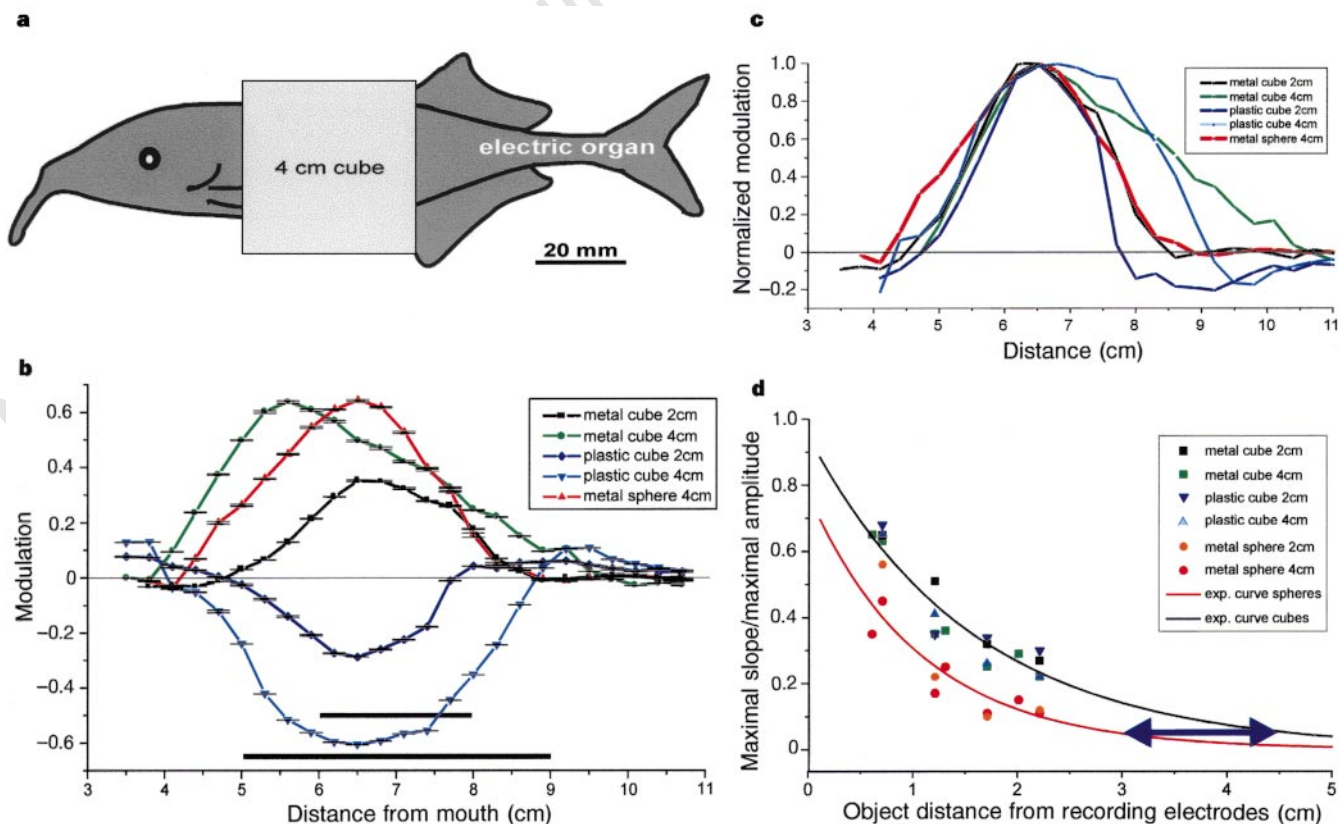


Figure 3 Electric image measurements. **a**, Fish with a cube positioned for electric image measurements. **b**, Electrical images projected by five different objects, 12 mm from the skin surface. Horizontal black bars mark the object position. **c**, Normalized electric images obtained from data shown in **(b)**. Curves were shifted horizontally to align rostral (left) slopes approximately. Note that the rostral slopes for all cube-images are similar, whereas the slope for the sphere (red curve) is less steep. **d**, Slope-to-amplitude ratios calculated for two metal spheres (red curve)

and four cubes (black curve) plotted against object distance. The two curves are extrapolated from data-fit functions⁵; their parameters are $y = 0.7658e^{-0.9249x}$, $r = -0.888$, $P = 0.0002$ (red curve) and $y = 0.9445e^{-0.6343x}$, $r = -0.928$, $P < 0.0001$. Values of r and P were obtained by using a linear transfer function method³⁰. The double arrow indicates the distance between curves when the sphere was 3 cm from the fish.

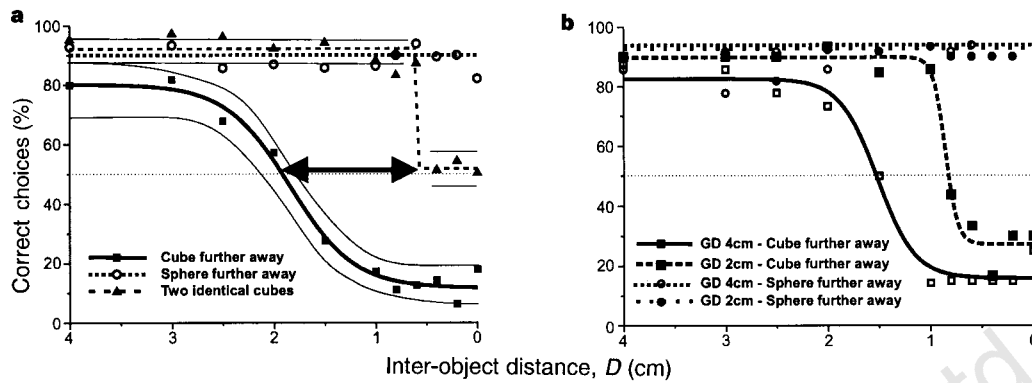


Figure 4 Psychometric functions for distance discrimination of a metal sphere and a metal cube, and for two identical metal cubes. **a**, Gate distance was fixed at 3 cm. Two curves are shown for the sphere/cube discrimination task: results obtained when either the cube (squares) or the sphere (circles) were further away. The double arrow marks the shift to the left of the curve fitted to the squares

relative to that obtained with two identical cubes (triangles). Thin lines indicate 95% confidence limits for the fitted functions. All curves are significantly different ($P < 0.05$). **b**, Psychometric functions obtained when a fish discriminated between a sphere and a cube at a gate distance of 2 cm (squares) or 4 cm (circles).

bears some resemblance to the mechanism that flies use to land on a target: the onset of deceleration is triggered when the ratio of the image expansion of the target on the retina to the image size reaches a critical value²⁰. To be independent of object parameters, the image expansion parameter is standardized by image size. Similarly, in our hypothesis about active electric imaging, the slope parameter is standardized by maximal amplitude, making the slope-to-amplitude ratio independent of object parameters such as size, impedance or form.

In conclusion, we found that electric fish can measure the distance of objects in complete darkness by means of active electrolocation. Distance discrimination is very accurate, as long as the geometrical forms of the edges of the objects being compared do not differ too strongly. Fish can perceive three-dimensional depth without time or spectral measurements even when the receptive surface is stationary. □

Methods

Discrimination training. Three individuals of the weakly electric African fish *Gnathonemus petersii* (standard lengths between 11 and 14 cm) were trained in a rectangular tank that was divided into two compartments (60 cm × 35 cm and 20 cm × 35 cm) by a coarse plastic mesh containing two gates 15 cm apart (Fig. 1c). For the electrolocation discrimination task, two test objects were mounted in the smaller compartment behind the left and right gates at a distance chosen in a pseudo-random manner. The test objects were solid aluminium cubes (volumes 125, 64, 27 or 8 cm³), plastic cubes (125, 64, 27 or 8 cm³), aluminium plates (5 cm × 5 cm × 2 cm), aluminium pyramids (64 cm³) and aluminium spheres (diameter 4 cm or 2 cm). In a food-rewarded two-alternative forced-choice procedure, animals were trained to swim through that gate behind which the object was located farther away (S+). Distance-discrimination thresholds (defined as 70% correct choices) were measured by keeping the gate distance of the closer object constant, and by reducing the distance between the second object and its corresponding gate in progressive steps, thus reducing the distance between the two objects (D in Fig. 1c). Each point of the psychometric functions determined in this manner was based on at least 150 decisions. Except for controls, experiments were conducted at low light intensities (0.75 lx).

Control experiments. Three types of control experiment were conducted. (1) To measure the effect of the dim illumination, five experiments were conducted in infrared light, which is invisible to mormyrids²⁸. Threshold curves thus obtained in the absence of vision, and with light present, were compared. There was no statistical difference between thresholds obtained with or without visible light ($P < 0.05$). Thus, even when vision was possible, the fish relied on active electrolocation to determine object distance. (2) To prove that fish were using active electrolocation for the required task, electrical noise (bandwidth 2–5 kHz, minimum noise amplitude = 70 mV cm⁻¹ (r.m.s.)) was played to the fish during the discrimination task. The two fish tested were unable to

discriminate object distances under these conditions and reached success rates of 50 ± 10%. (3) To prove that fish were not making a comparison by electrolocating the two objects simultaneously, a thin glass plate that was impenetrable to electrolocation signals was mounted between the two objects, making it impossible for the fish to image both at the same time. The performances of the fish were statistically identical ($P < 0.05$) with and without the glass divider present. Psychometric functions were compared by transforming the sigmoid curves into linear functions, recalculating data points according to this transfer function and comparing slopes with a modified Student's *t*-test as described by Zar²⁹.

Measurement of electric images. The electric images of the same objects that were used in the behavioural experiments were measured experimentally along the lateral electroreceptive surface of the fish (Fig. 3a). Three *G. petersii* were sedated with Hypnodil (metomidate R7315; Janssen Veterinary Division; 5 mg l⁻¹ aquarium water) and supported in the middle of a 40 cm × 20 cm recording tank. Under Hypnodil, a fish discharges its electric organ at a regular slow rhythm. Electric organ discharges (EODs) were recorded with a pair of copper wire electrodes insulated except at the tip (distance between electrodes, 1 mm). To avoid capacitive coupling, these electrodes were individually shielded and connected separately to the two inputs of an Axoclamp 2A amplifier. The two outputs of the amplifier were connected to a differential amplifier (Tektronix 5A22N) in a Tektronix 5223 digitizing oscilloscope. The recorded EOD signal was transferred to a computer hard disc by using ACQUIS1 software (G. Sadoc, C.N.R.S.). The electrode pair was moved in a straight line, in steps of 3 mm, along the side of the fish at the height of the lateral line, at a constant distance of 1 mm (5 mm in one fish) from the skin surface. At each position, ten records of the local EOD were averaged and the peak-to-peak amplitude of the EOD was determined. Control measurement series were made in the absence of any object between each trial series. Images of several types of objects located at seven different distances from the fish's surface were measured. The relative modulation of the EOD peak-to-peak amplitude was defined as the ratio between the change produced by the object and the amplitude in the absence of an object. The electric image of an object was defined as the profile of the relative modulation along the fish's body (Fig. 3b)⁷. For each electrical image, we determined the maximal image amplitude and maximal image slope values. The maximal value of the rostral slope of the image was divided by the maximal image amplitude to obtain the slope-to-amplitude ratio for each image.

Received 16 June; accepted 20 August 1998.

- Collett, T. S. & Harkness, L. I. K. in *Analysis of Visual Behaviour* (eds Ingle, D. J., Goodale, M. A. & Mansfield, J. W.) 111–175 (MIT Press, 1982).
- Lissmann, H. W. & Machin, K. E. The mechanism of object location in *Gymnarchus niloticus* and similar fish. *J. Exp. Biol.* **35**, 451–486 (1958).
- von der Emde, G. in *The Physiology of Fishes* (ed. Evans, D. H.) 313–343 (CRC, Boca Raton, 1998).
- Bastian, J. in *Comparative Perception* (eds Stebbins, W. C. & Berkeley, M. H.) 35–89 (Wiley, New York, 1989).
- Schwarz, S. Diplomarbeit, Institut für Zoologie, Universität Bonn (1997).
- Heiligenberg, W. Electrolocation of objects in the electric fish *Eigenmannia* (Rhamphichthyidae, Gymnotoidei). *J. Comp. Physiol.* **87**, 137–164 (1973).
- Caputi, A., Budelli, R., Grant, K. & Bell, C. C. The electric image in weakly electric fish. II Physical images of resistive objects in *Gnathonemus petersii*. *J. Exp. Biol.* **201**, 2115–2128 (1998).

8. Rasnow, B. The effects of simple objects on the electric field of *Apterionotus*. *J. Comp. Physiol. A* **178**, 397–411 (1996).
9. Howard, I. P. & Rogers, B. J. *Binocular Vision and Stereopsis* (Oxford Univ. Press, New York, 1995).
10. Collett, T. Stereopsis in toads. *Nature* **267**, 349–351 (1977).
11. Kral, K. & Poteser, M. Motion parallax as a source of distance information in locusts and mantids. *J. Insect Behav.* **10**, 145–163 (1997).
12. Lehrer, M., Wehner, R. & Srinivasan, M. V. Motion cues provide the bee's visual world with a third dimension. *Nature* **332**, 356–357 (1988).
13. Schuij, A. & Hawkins, A. D. Acoustic distance discrimination by the cod. *Nature* **302**, 143–144 (1983).
14. Bleckmann, H. *Reception of Hydrodynamic Stimuli in Aquatic and Semiaquatic Animals* (Gustav Fischer, Stuttgart, 1994).
15. Atema, J. Eddy chemotaxis and odor landscapes: exploration of nature with animal sensors. *Biol. Bull.* **191**, 129–138 (1996).
16. Moller, P., Serrier, J., Belbenoit, P. & Push, S. Notes on the ethology and ecology of the Swashi river mormyrids (Lake Kainji, Nigeria). *Behav. Ecol. Sociobiol.* **4**, 357–368 (1979).
17. von der Emde, G. The sensing of electric capacitances by weakly electric mormyrid fish: effects of water conductivity. *J. Exp. Biol.* **181**, 157–173 (1993).
18. Tippler, A. *Physik* (Spektrum Akademischer, Heidelberg, 1994).
19. von der Emde, G. & Bleckmann, H. Finding food: senses involved in foraging for insect larvae in the electric fish, *Gnathonemus petersii*. *J. Exp. Biol.* **201**, 969–980 (1998).
20. Wagner, H. Flow-field variables trigger landing in flies. *Nature* **297**, 147–148 (1982).
21. Hassan, E. S. in *The Mechanosensory Lateral Line. Neurobiology and Evolution* (eds Coombs, S., Görner, P. & Münz, H.) 217–228 (Springer, Berlin, 1989).
22. Bleckmann, H., Tittel, G. & Blübaum-Gronau, E. in *The Mechanosensory Lateral Line. Neurobiology and Evolution* (eds Coombs, S., Görner, P. & Münz, H.) 501–526 (Springer, Berlin, 1989).
23. Harkness, L. Chameleons use accommodation cues to judge distance. *Nature* **267**, 346–349 (1977).
24. Hopkins, C. D. Temporal structures of non-propagated electric communication signals. *Brain Behav. Evol.* **28**, 43–59 (1986).
25. Suga, N., Butman, J. A., Teng, H., Yan, J. & Olsen, J. F. in *Active Hearing* (eds Flock, A., Otosson, D. & Ulfendahl, M.) 13–30 (Pergamon, New York, 1995).
26. Schnitzler, H.-U., Menne, D. & Hackbarth, H. in *Time Resolution in Auditory Systems* (ed. Michelsen, A.) 180–204 (Springer, Berlin, 1985).
27. Dear, S. P., Simmons, J. A. & Fritz, J. A possible neuronal basis for representation of acoustic scenes in auditory cortex of the big brown bat. *Nature* **364**, 620–623 (1993).
28. Cialo, S., Gordon, J. & Moller, J. Spectral sensitivity of the weakly discharging electric fish *Gnathonemus petersii* using its electric organ discharges as the response measure. *J. Fish Biol.* **50**, 1074–1087 (1997).
29. Zar, J. H. *Biostatistical Analysis* (Prentice Hall, Englewood Cliffs, 1984).
30. Hoerl, A. E. Jr in *Chemical Business Handbook* (ed. Perry, J. H.) 20–50 (McGraw-Hill, London, 1954).

Acknowledgements. The behavioural experiments and the analysis of the electric images were performed by S.S. during work for his diploma thesis. We thank H. Bleckmann for providing laboratory space and for his continuous support throughout this study; C. C. Bell, H. Bleckmann, J. Mogdans, S. F. Perry, E. Schaeffel and H. Wagner for critically reading the manuscript and helpful discussions; C. Gutzen for help with the figures; and W. Alt for statistical advice. G.v.d.E. is a recipient of a Heisenberg stipend of the DFG. This work was financed partly by a research grant from the EC to K.G. by the Franco-German international exchange programme PROCOPE, by the Franco-Uruguayan exchange programme ECOS and by a doctoral fellowship to L.G. from the French Ministry of Foreign Affairs.

Correspondence and requests for materials should be addressed to G.v.d.E. (e-mail: unb308@uni-bonn.de).

Seeing biological motion

Peter Neri*, M. Concetta Morrone† & David C. Burr‡

* University Laboratory of Physiology, Parks Road, Oxford OX1 3PT, UK

† Istituto di Neurofisiologia del CNR, Via S. Zeno 51, Pisa 56127, Italy

‡ Department of Psychology, University of Florence, Florence 50125, Italy

One of the more stunning examples of the resourcefulness of human vision is the ability to see 'biological motion', which was first shown¹ with an adaptation of earlier cinematic work²: illumination of only the joints of a walking person is enough to convey a vivid, compelling impression of human animation, although the percept collapses to a jumble of meaningless lights when the walker stands still. The information is sufficient to discriminate the sex and other details of the walker^{3,4}, and can be interpreted by young infants⁵. Here we measure the ability of the visual system to integrate this type of motion information over space and time, and compare this capacity with that for viewing simple translational motion. Sensitivity to biological motion increases rapidly with the number of illuminated joints, far more rapidly than for simple motion. Furthermore, this information is summed over extended temporal intervals of up to 3 seconds (eight times longer than for simple motion). The steepness of the summation curves indicates that the mechanisms that analyse biological motion do not integrate linearly over space and time with constant efficiency, as may occur for other forms of complex motion⁶, but instead adapt to the nature of the stimulus.

Biological motion was produced on a video display by an adaptation of a standard cyclic algorithm⁷ that emulates the

motion of the 11 main joints of a person walking on a treadmill. Subjects were required either to detect the presence of the walker or to discriminate the direction of walking, in the presence of variable amounts of dynamic random noise. Similar tasks were performed for simple translational motion, for which a random pattern of dots was continuously displaced horizontally within a window of dimensions similar to that of the walker. We adapted the standard biological-motion technique so that each point had a 'limited lifetime' of two frames, after which it disappeared and was redrawn in another randomly chosen position (see Fig. 1 and Methods). This allowed for dynamic undersampling of the entire dot pattern, ensuring that, even at the lowest sampling rates, all 11 joints were likely to be represented during the 1,200-ms exposure time.

Figure 2 shows how sensitivity (expressed as maximum tolerable noise) for detection and direction discrimination varied with the number of displayed points for the two types of motion. For translational motion, sensitivity for both detection and discrimination increased with dot number at a very similar rate, almost linearly for both subjects tested (log-log slope is roughly at unity). For biological motion, the summation curves for detection were very similar to those for detection of translation, in both slope and absolute sensitivity. But the direction-discrimination curves were far steeper, with log-log slopes of about 3 or more (indicating a cubic or higher relationship).

Figure 3 shows how sensitivity to the walker varied with exposure time (temporal summation). As before, we used a limited-lifetime paradigm, with six dots displayed. Sensitivity to both simple and biological motion increased with time, first rapidly then more gradually. In comparable studies, it was thought that the initial rapid increase reflects physiological summation, whereas the gradual phase reflects 'probability summation' (a statistical improvement based on recruitment of independent detectors rather than summation within a single unit⁸). The intersection of these two curves gives an estimate of the time constant of the

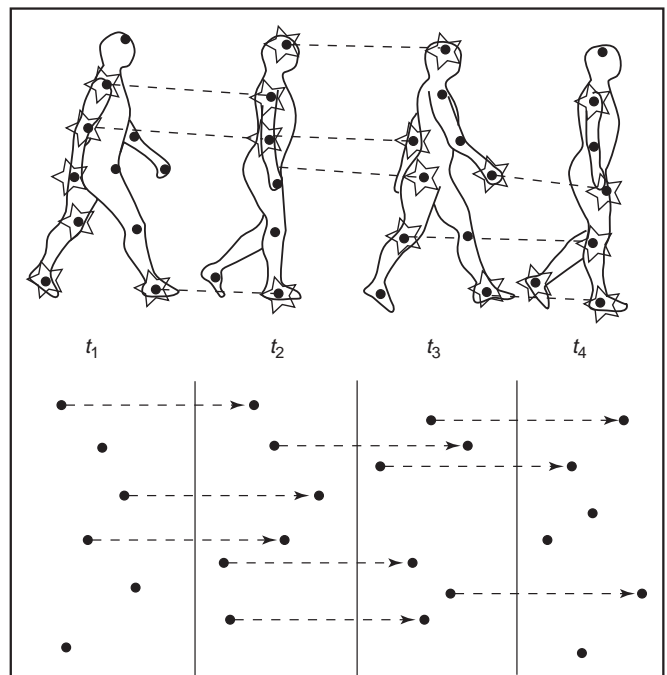


Figure 1 The limited-lifetime technique for studying the ability to see biological motion (upper figures) and translational motion (lower figures), for six-dot sampling (over a two-frame running average). The starred points of the walker indicate those that are actually in motion; the others, the possible positions to be sampled. Half of the dots move from frames 1 to 2, and the other half from frames 2 to 3. The starred points sometimes undergo occlusion (when required by the algorithm⁷), and are not visible at these times.